

Roughening of Stepped Metal Surfaces

Marcel den Nijs and Eberhard K. Riedel

Department of Physics, University of Washington, Seattle, Washington 98195

and

E. H. Conrad and T. Engel

Department of Chemistry, University of Washington, Seattle, Washington 98195

(Received 8 July 1985)

A generic phase diagram is proposed for stepped ($11m$) surfaces of fcc metals, which describes the roughening transition and subsequent changes of the nature of the rough phase in terms of a sequence of universal values for the roughness parameter $x_1(T, m)$. From a detailed analysis of atom-beam diffraction profiles of Ni(115), for $100 \text{ K} < T < 900 \text{ K}$, it is concluded that Ni(115) is rough in this temperature interval. The roughening temperatures of Ni(113) and Ni(001) are predicted to be $200 \pm 50 \text{ K}$ and well above 420 K , respectively. Near 420 K , islands appear in the rough (115) surfaces in addition to the meandering steps.

PACS numbers: 68.20.+t, 64.60.Fr, 68.40.+e, 82.65.Dp

Extensive studies in recent years have shown that surface defects can have an appreciable effect on a wide range of structural and electronic properties of surfaces and interfaces as well as on the chemical reactivity of surfaces. Here we report the first evidence for the roughening^{1,2} of stepped ($11m$) metal surfaces, which is obtained from the detailed analysis of atom-beam diffraction (ABD) line shapes. Specifically, we propose a generic phase diagram for ($11m$) surfaces and, by combining this with our experimental results for Ni(115), we conclude the following: (i) The Ni(115) surface is rough in the experimentally studied temperature interval $100 \text{ K} < T < 900 \text{ K}$; the roughening temperature of Ni(115) is $T_R < 50 \text{ K}$. (ii) Ni(113) is predicted to roughen at $T_R = 200 \pm 50 \text{ K}$, and all other Ni($11m$) faces ($m > 1$) at lower temperatures. (iii) The roughening temperature of Ni(001) is well above 420 K . (iv) Dips in the diffraction intensity observed for Ni(115) and Cu($11m$) surfaces^{3,4} near 420 K reflect island formation as characteristic of the roughening of the (001) surfaces.

Figures 1(a)–1(c) show typical configurations of stepped ($11m$) surfaces for three temperature regimes. In the ordered phase, Fig. 1(a), the steps are equally spaced and do not meander. The two basic fluctuations are the meandering of the steps, Fig. 1(b), and the formation of stacked or nested islands, Fig. 1(c). The ordered phase is stable only if the range of the interactions is such that steps repel each other. In that case Fig. 1(a) characterizes the surface until the roughening transition at nonzero $T_R(11m)$. At $T_R(11m)$ the entropy gained by meandering of the steps becomes larger than the energy lost by placing the steps closer to each other. The roughening transition is a Kosterlitz-Thouless (KT) transition.¹ Above $T_R(11m)$, see Fig. 1(b), the degree of roughness increases with temperature and is characterized by the roughness parameter $x_1(T, m)$ to be defined below. The steps have a fractal structure (like coastlines), which is

geometrically characterized by a set of fractal dimensions; i.e., the correlation length is infinite and the correlation functions decay as inverse powers with critical exponents determined by those fractal dimensions.

Although no more phase transitions take place for $T > T_R(11m)$, the temperature behavior of $x_1(T, m)$ re-

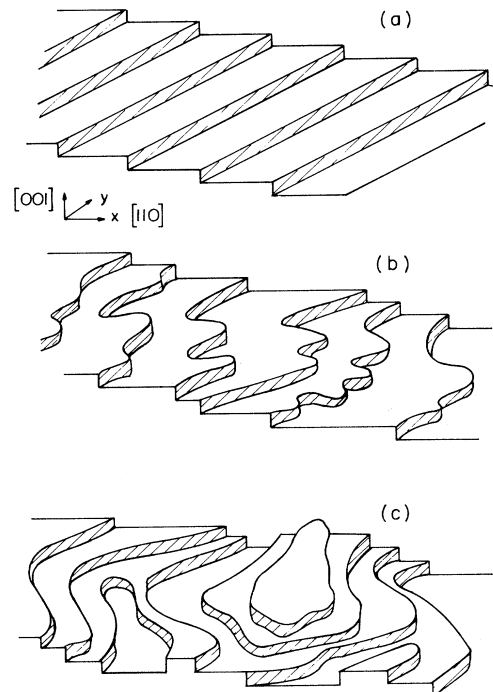


FIG. 1. Configurations of stepped ($11m$) surfaces with increasing temperature. (a) Ordered phase. (b) Rough phase with meandering steps. (c) Rough phase above $T_R(001)$ with nested islands.

flects roughening transitions in other $(11m)$ faces. For example, the roughening of the (113) face at $T_R(113) > T_R(115)$ shows up in the roughness of the (115) face as the characteristic temperature below which the steps, although meandering, do not approach each other by distances less than the (113) terrace width. The roughening of the flat (001) face takes place at an even higher temperature. At $T_R(001)$ the meander entropy becomes large enough that the free energy needed to create steps vanishes. Islands are formed. These islands are nested and have boundaries that, like the meandering steps, have a fractal structure. The roughening of the (001) face is reflected in the roughness of the $(11m)$ face as the characteristic temperature where, in addition to meandering steps, islands appear on the (001) terraces. Here the character of the rough phase changes from that of Fig. 1(b) to that of Fig. 1(c).

Our task is to determine how the experimental temperature interval fits into this generic sequence of characteristic surface configurations. First we show that the roughness parameter $x_1(T, m)$ assumes specific universal values at the roughening temperature and the other characteristic temperatures. Next we describe how $x_1(T, m)$ can be extracted from ABD line shapes. Finally we discuss our results for Ni(115).

The theory of roughening transitions is well known.¹ Our generalization to stepped $(11m)$ surfaces has strong similarities with the theory of commensurate-incommensurate phase transitions⁵ (where domain walls play the role of the steps) and with the theory of crystal

shapes.⁶

As usual, we describe the surface by a solid-on-solid (SOS) model. The surface is characterized by the heights of columns of atoms by assigning height variables h_r to the sites $r = (x, y)$ of a two-dimensional lattice. Since the (001) faces of Ni and Cu are body centered, they are described by the body-centered solid-on-solid (BCSOS) model,⁷ with "integer lattice sites" (n_x, n_y) and "half-integer sites" $(n_x + \frac{1}{2}, n_y + \frac{1}{2})$, in units of the nearest-neighbor distance a_0 ; the x and y axes are along the $[110]$ and $[\bar{1}10]$ directions. The height variable h_r , in units of $a_0/\sqrt{2}$, takes integer values at the integer sites and half-integer values at the half-integer sites. The heights of nearest-neighbor columns are restricted to differ by a half integer. The forces between the particles are represented by an interaction $V(h_r - h_{r'}, r - r')$ between columns.

First consider the (001) surface. In the rough phase, there is no limit to the height fluctuations; the height-height correlation function diverges logarithmically.¹ For $R \gg 1$,

$$\langle (h_r - h_0 - x/m)^2 \rangle = (x_1/\pi^2) \ln(R), \quad (1)$$

with $R^2 = (x/N_m)^2 + (y/2)^2$, where $m = \infty$ and $N_\infty = 2$ for the (001) face. $x_1 = x_1(T, m)$ is the roughness parameter mentioned above. As a result of the long-wavelength fluctuations the discreteness of the steps is irrelevant; the rough phase is described by the Gaussian model.¹ To determine the universal values of the roughness parameter at $T_R(11m)$ for different m , consider the following version of the sine-Gordon model:

$$Z = \sum_{\{\phi_r\}} \exp \left[\sum_{r, r'} V(\phi_r - \phi_{r'}, r - r') \right] \prod_r \sum_{N_r} z^{N_r^2} \exp[2\pi i (\phi_r + x) N_r]. \quad (2)$$

The ϕ_r are continuous variables, subject to the weight function $\exp(2\pi i \phi_r N_r)$ with $N_r = 0, \pm 1, \pm 2, \dots$, which favors integer values of ϕ_r at integer sites and half-integer values at half-integer sites.⁸ The significance of the fugacity parameter z is that it allows us to identify the sine-Gordon operator that drives the roughening transition. At $z = 1$ the model becomes the BCSOS model, at $z = 0$ the Gaussian model, and for small z a sine-Gordon model. Above the roughening transition the BCSOS model flows under renormalization towards the Gaussian model, such that $x_1 = \pi/K_G$, with K_G the fixed-point value of the Gaussian coupling constant.¹ In the rough phase and in the scaling region around the roughening transition the BCSOS model belongs to the same universality class as the sine-Gordon model,

$$Z = \sum_{\{\phi_r\}} \exp \left\{ \sum_{\langle r, r' \rangle} K_G (\phi_r - \phi_{r'})^2 + \sum_r \sum_N 2z_N \cos[2\pi N (\phi_r + x + x/m)] \right\}, \quad (3)$$

with $N = 0, 1, 2, \dots$, nearest-neighbor summation $\langle r, r' \rangle$, and $m = \infty$ for the (001) crystal face. The roughening transition of the BCSOS model is driven by the $\cos(4\pi\phi)$ operator, rather than $\cos(2\pi\phi)$.⁹ On a technical level, this is due to the modulation in the $\cos(2\pi\phi)$ operator, which implies that this operator is irrelevant. On a more intuitive level, this is due to the doubling of the unit cell in the BCSOS model with respect to the conventional SOS model.¹ As a rule of thumb, the roughening transition is driven by the sine-Gordon operator with the lowest wave number N in Eq. (2) that is not modulated at any of the lattice sites.

Crucial for our discussion is the result¹ that K_G and therefore the roughness parameter x_1 take a universal value at $T_R(001)$. In our notation $x_1^{(R)} = \frac{1}{2}$. At $T_R(001)$ the $\cos(4\pi\phi)$ operator becomes marginal, i.e., its critical dimension is $x_N = x_1 N^2 = 2$ with $N = 2$.^{8,9}

Stepped (11*m*) surfaces, Fig. 1(a), are described by our imposing a finite step density in the BCSOS model, $\phi_{L,y} = \phi_{0,y} + L/m$ and $\phi_{L+1/2,y} = \phi_{1/2,y} + L/m$, with *L* the length of the surface in the *x* direction (such that *L/m* is an integer). Periodic boundary conditions are restored in Eq. (2) by the introduction of new variables $\tilde{\phi}_r = \phi_r - x/m$. This redirects the column direction to the new surface normal. As before, the BCSOS model belongs to the same universality class as the sine-Gordon model, but now with different phase factors $m < \infty$ in Eq. (3). The roughening of the (11*m*) face is driven by a sine-Gordon operator with a different wave number, *N_m*, because of the different periodicity of the ordered phase. According to our rule of thumb, *N_m* is equal to the smallest integer satisfying the equation $N_m(m^{-1} + 1) = 2 \pmod{2}$. Hence, $N_m = m$ when *m* is odd and $N_m = 2m$ when *m* is even. Since at the roughening transitions $x_N = x_1 N_m^2 = 2$, it follows that x_1 takes the universal values $x_1^{(R)} = 2/N_m^2$ at $T_R(11m)$. For example, at the roughening temperature of the (115) face, $x_1^{(R)} = \frac{2}{25}$; and at $T_R(113)$, $x_1^{(R)} = \frac{2}{9}$; both values are much smaller than $x_1^{(R)} = \frac{1}{2}$ at $T_R(001)$. In SOS models where the step height is not restricted, the roughness continues to increase with temperature. In the BCSOS model, where only steps of height $\pm \frac{1}{2}$ are allowed, x_1 has an upper bound, $x_1 = \frac{3}{2}$.¹⁰

We can now draw a generic (*T*, 1/*m*) phase diagram for (11*m*) metal surfaces; see Fig. 2. The solid lines represent ordered low-temperature phases, Fig. 1(a). Everywhere else the surface is rough and characterized by $x_1(T, m)$. Lines of constant x_1 can be drawn schematical-

ly.¹¹ x_1 assumes the universal values $x_1^{(R)}$, when $T = T_R(11m)$, and $x_1 = x_1^{(R)}/2$, when the ordered phases (solid lines) are approached as a function of *m* at fixed $T < T_R(11m)$. The latter follows from the theory of commensurate-incommensurate transitions.⁵ The other features of the lines of constant x_1 are not universal. $x_1(T, m)$ behaves very nonanalytically in the limit of zero temperature if the range of the step-step interaction is sufficiently long so that many ordered phases are stable (including those with two or more alternating step-step distances). This would lead to a so-called devil's staircase in the phase diagram at $T = 0$.¹² At higher temperatures $x_1(T, m)$ smoothens out. The line $x_1 = \frac{1}{2}$ gives the characteristic temperature where islands appear in the rough (11*m*) surfaces.

ABD experiments measure the scattering function $S(q, Q)$, which is the Fourier transform of the correlation functions $G_Q(r) = \langle \exp[2\pi i Q(h_r - h_0)] \rangle$.^{13,14} Here $q = (q_x, q_y)$ denotes the component of the momentum transfer parallel to the surface and *Q* the component perpendicular to the surface. Along the diffraction rods the peak width exhibits maxima and minima as a function of *Q* as a result of interference between steps.¹⁴ $S(q, Q)$ is periodic in *Q*, with period 2. $Q = 0 \pmod{2}$ defines the Bragg angles where the peak width is minimal, and $Q = 1 \pmod{2}$, the anti-Bragg angles where the peak width is maximal. ABD is insensitive to the corrugation of the (001) plane, and therefore no periodicity of $S(q, Q)$ in q_y is seen and the observed spacing of the diffraction rods in q_x is 2 times larger.⁴

The line shapes indicate directly whether the surface is ordered or rough. The correlations decay exponentially in the ordered phase and as an inverse power in the rough phase. In the rough phase, for $R \gg 1$,

$$G_Q(r) = A_0 R^{-2x_Q} e^{2\pi i Q x / m}, \tag{4}$$

with $x_Q = x_1 k^2$, where $k = Q \pmod{2}$ in the interval $-1 < k < 1$, and with $R^2 = (x/N_m)^2 + (y/2)^2$.⁴

For Ni(115) we find power-law behavior at all temperatures $100 \text{ K} < T < 900 \text{ K}$ and obtain x_Q from power-law fits using log-log plots.⁴ Such plots yield the value of x_Q inside a window bounded at small *q* as a result of the instrument width and finite domain size, and at large *q* as a result of the overlap between diffraction peaks. Both this window and the diffraction sensitivity become optimal at the anti-Bragg angles. We checked that at the anti-Bragg angles $Q = 1, 3, 5$, the values for x_Q are consistent for incident beams perpendicular and parallel to the steps. To minimize inelastic effects (Debye-Waller), the value of x_1 was determined from data at the anti-Bragg angle $Q = 3$.⁴ Although asymptotically x_Q , as defined below Eq. (4), has cusps at the anti-Bragg angles, it rounds off as a result of finite-size effects such that x_Q becomes insensitive to *Q* and $x_Q = x_1$ near $Q = 1 \pmod{2}$.⁴

Figure 3 shows x_1 for Ni(115) as a function of temperature. x_1 is roughly linear in the interval

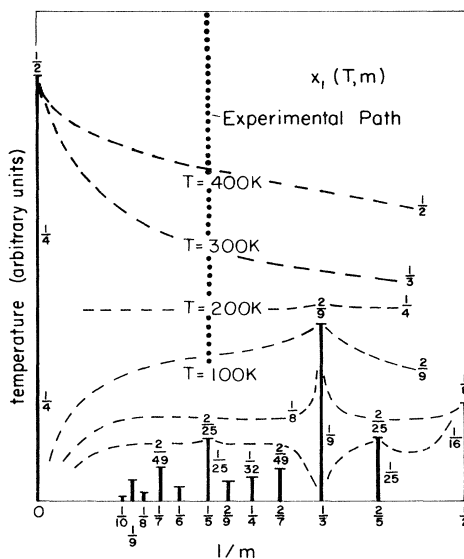


FIG. 2. Generic phase diagram for (11*m*) metal surface. The solid lines represent ordered phases. Along the dashed lines the roughness $x_1(T, m)$ is constant. The dotted line represents the experimental path for Ni(115).

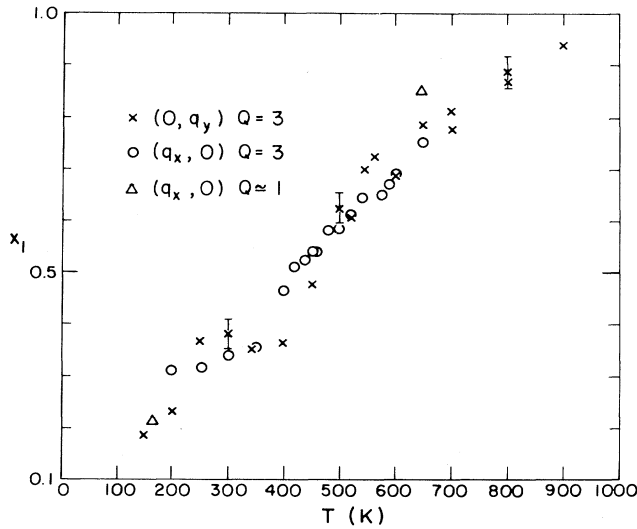


FIG. 3. Roughness parameter x_1 vs temperature for Ni(115) from line-shape analysis of the specular peak close to anti-Bragg angles Q for scattering parallel and perpendicular to the direction of the steps.

100 K $< T < 900$ K, and larger than $x_1^{(R)} = \frac{2}{25}$. Therefore, Ni(115) is above its roughening temperature. We estimate that $T_R(115)$ is less than 50 K. The value $x_1^{(R)} = \frac{2}{9}$, indicating the roughening of Ni(113), is at the lower end of the temperature interval; we predict that $T_R(113)$ is approximately 200 ± 50 K. The value $x_1^{(R)} = \frac{1}{2}$, indicating the roughening of Ni(001), occurs at $T = 420 \pm 50$ K. Here the topology of the surface changes from that of Fig. 1(b) to that of Fig. 1(c). Because of the cusp at $1/m = 0$ in the $x_1 = \frac{1}{2}$ line in Fig. 2,¹¹ the roughening of Ni(001) takes place at higher temperature. Since the height of the cusp is unknown, we can infer only that $T_R(001) > 420$ K. A value of $T_R(001) = 700$ K would imply that the energy required to create a step in the (001) face is of the order of 500 K per unit length a_0 .⁴ Direct measurements of $T_R(113)$ and $T_R(001)$ are under way.

Finally, we comment on recent work on Cu(11 m) faces,

with $m = 3, 5, 7$.^{2,3} The diffraction intensity for Ni(115) drops near $T = 420$ K.⁴ We know from our line-shape analysis that this drop in intensity reflects the (001) roughening. Similar drops have been observed with ABD for Cu(11 m) surfaces, all at comparable temperatures $T = 420 - 500$ K.³ Assuming similar energetics for Cu and Ni, we interpret these results to reflect the roughening of the Cu(001) surface as well. This conclusion contradicts a recent suggestion (based on studies of intensity only) by Villain, Grempele, and Lapujoulade² that these drops in intensity are associated with the roughening of the (11 m) surface itself. The step energy is considerably smaller than that assumed by them.

This work was supported in part by the National Science Foundation under Grants No. DMR 83-19301 and No. CHE 81-09067.

¹For a review, see J. D. Weeks, in *Ordering of Strongly Fluctuating Condensed Matter Systems*, edited by T. Riste (Plenum, New York, 1980), p. 293.

²J. Villain, D. R. Grempele, and J. Lapujoulade, *J. Phys. F* **15**, 809 (1985).

³J. Lapujoulade, J. Perreau, and A. Kara, *Surf. Sci.* **129**, 59 (1983).

⁴E. H. Conrad, R. M. Aten, D. S. Kaufman, L. R. Allen, T. Engel, M. den Nijs, and E. K. Riedel, to be published.

⁵V. L. Pokrovsky and A. L. Talapov, *Phys. Rev. Lett.* **42**, 65 (1979); see also J. Villain and M. B. Gordon, *Surf. Sci.* **125**, 1 (1981).

⁶C. Rottman, M. Wortis, J. C. Heyraud, and J. J. Metois, *Phys. Rev. Lett.* **52**, 1009 (1984).

⁷H. van Beijeren, *Phys. Rev. Lett.* **38**, 993 (1977).

⁸L. P. Kadanoff, *Ann. Phys. (N.Y.)* **120**, 39 (1979).

⁹H. J. F. Knops, *Ann. Phys. (N.Y.)* **128**, 448 (1980).

¹⁰M. den Nijs, *Phys. Rev. B* (to be published).

¹¹See also F. D. M. Haldane, *Phys. Rev. Lett.* **45**, 1358 (1980).

¹²Compare, e.g., P. Bak, *Rep. Prog. Phys.* **45**, 587 (1982).

¹³G. Blatter, *Surf. Sci.* **145**, 419 (1984).

¹⁴M. Henzler, in *Electron Spectroscopy for Surface Analysis*, edited by H. Ibach (Springer, Berlin, 1979), p. 117.